RSC Advances

PAPER

View Article Online
View Journal | View Issue

Check for updates

Cite this: *RSC Adv.*, 2024, **14**, 15293

Effect of incorporating white pepper (*Piper nigrum* L.) oleoresin on starch/alginate films

Olga Lucía Torres Vargas, * Iván Andrés Rodríguez Agredo and Yessica Viviana Galeano Loaiza

Received 1st February 2024
Accepted 7th May 2024

DOI: 10.1039/d4ra00821a

rsc.li/rsc-advances

The development of films based on natural components has demonstrated their potential for food preservation. In this research, the effect of the inclusion of white pepper oleoresin (WPO) in a film made from cassava starch and sodium alginate (FWPO) on the antimicrobial, physicochemical, mechanical, optical, and structural properties was evaluated. The films were formulated with different concentrations of WPO (0.0, 0.5, 1.0 and 1.5%). The results obtained indicated that the incorporation of WPO in the film increased the antioxidant activity against the 1,1-diphenyl-2-picryl-hydrazyl radical (DPPH), and an inhibitory effect against *Escherichia coli* and *Staphylococcus aureus* bacteria was also observed. Elongation at break (EB), water vapor permeability (WVP), moisture content, solubility, and luminosity (L^*) decreased significantly ($p < 0.05$) with the addition of WPO. On the other hand, the tensile strength (TS), the value of b^* (tendency toward yellow) and the opacity increased. Scanning electron microscopy (SEM) images showed a smooth, uniform appearance, and continuous dispersion between cassava starch, alginate and WPO. FTIR spectra showed the interactions between the film components. X-ray diffraction (XRD) patterns showed that the addition of WPO did not affect the structural stability of the films. The results obtained indicate the possible use of WPO in the packaging of food products, contributing to the improvement of food quality and safety.

Open Access Article. Published on 13 May 2024. Downloaded on 2/12/2026 11:27:03 PM.
This article is licensed under a Creative Commons Attribution-NonCommercial 3.0 Unported Licence.

1. Introduction

Obtaining biodegradable materials from renewable sources and reducing the use of plastic packaging not only contribute to the goal of preserving the environment in the packaging industry,[1] but also address crucial concerns related to microbial contamination and lipid oxidation. These problems represent significant threats to public health, and for these reasons research is focused on compounds that exert antioxidant and/or antimicrobial activity.[2] Therefore, one of the great challenges currently facing researchers, in addition to environmental problems, is creating mechanisms that control food contamination by the action of pathogenic microorganisms.

Consumer demand for healthier and safer foods has led to the development of new preservation techniques. Traditionally, antimicrobial/antioxidant agents were added directly to foods to prevent contamination. Direct application of these agents to foods has limited effects because the active ingredients are quickly neutralized and can worsen the sensory properties of foods.[3] Therefore, films containing antibacterial or antioxidant agents may be more effective, allowing the bioactive agents to be released gradually over time.[4]

Food safety reports from the World Health Organization (WHO) indicate that access to safe and nutritious food in sufficient quantities is critical to sustaining life and promoting good health. Unsafe food containing harmful bacteria, viruses, parasites, or chemicals causes more than 200 diseases, ranging from digestive problems to cancer.[5] Therefore, the replacing of conventional petroleum-based packaging materials with biodegradable polymers-formulated antimicrobial films has become a topic of great interest for researchers in recent years.[6]

Currently, numerous studies have focused on the development of films based on starch, the most abundant biopolymer in nature, which is low cost (lower than polyethylene), widely available, biodegradable, edible, tasteless, colorless, and easy to use in technological processes.[7] Biopolymers formulated with cassava starch have shown excellent properties in obtaining flexible and extensible films with homogeneous and smooth surfaces.[8]

In addition, sodium alginate (AS) has attracted particular interest due to its commercial availability, biodegradability, and non-toxicity.[9] The colloidal nature of alginate gives it thickening, stabilizing, good film-forming, and suspending properties, characteristics that make it suitable as a biodegradable film-forming material.[10]

On the other hand, by solvent extraction from the peeled fruits white peppers, white pepper oleoresin (*Piper nigrum* L.) is obtained, which is widely used in the food industry because it

Group of Research on Agro-industrial Sciences, Interdisciplinary Science Institute, Food Engineering Laboratory, Universidad del Quindío, Cra. 15# 12 N, Armenia, Quindío, 630004, Colombia. E-mail: oltorres@uniquindio.edu.co

© 2024 The Author(s). Published by the Royal Society of Chemistry

Open Access Article. Published on 13 May 2024. Downloaded on 2/12/2026 11:27:03 PM. This article is licensed under a Creative Commons Attribution-NonCommercial 3.0 Unported Licence.

has strong antimicrobial activity, preserves its flavor, pungency, and functional properties, making it one of the most widely used spices worldwide.[11] WPO is a viscous liquid that has a slight spicy taste, with a characteristic peppery aroma, and is associated with several health benefits, such as anti-inflammatory, anticancer, antidiabetic, antimicrobial, antioxidant, and antifungal.[12–14]

Tween 80 is a nonionic surfactant commonly used as an emulsifier in the food and pharmaceutical industry.[15] The FDA (Food and Drug Administration)[16] granted Tween 80 generally recognized as safe (GRAS) status, and according to CXS-192 (ref. 17) its maximum allowable dose as an additive is 5000 mg kg^{-1}. However, at high concentrations, some studies have suggested that it may have adverse health effects.[15,18,19]

Consequently, the combination of biodegradable polymers with bioactive compounds to obtain films has become a promising technology for the food industry. Some of these combinations can improve the physical, mechanical, and barrier properties of the film, providing antimicrobial and antioxidant characteristics, which allow prolonging shelf life, maintaining quality, and improving the organoleptic properties of coated containers or foods.[20]

Therefore, the objective of this work was to evaluate the effect caused by the inclusion of white pepper oleoresin in a film made from cassava starch and sodium alginate on its antimicrobial, physicochemical, mechanical, optical and structural properties.

2. Materials and methods

2.1 Raw material

White pepper oleoresin (*Piper nigrum* L.) was purchased from Tecnas S. A., Colombia. Cassava starch (molecular weight: 2.169 × 10^7 g mol^{-1}) (TAPIOCA STARCH – 70000131LG) was purchased from Ingredion (Cali, Colombia). Alginate (molecular weight: 1.43 × 10^5 g mol^{-1}), $CaCl_2$ (molecular weight: 110.99 g mol^{-1}), glycerol, Tween 80, and the different reagents necessary for the physical and microbiological characterization of the formulated films were acquired from Merck in Colombia.

The bacterial strains *S. aureus* (ATCC 25923) and *E. coli* (ATCC 25922) were obtained from the culture collection of the Molecular Immunology Research Group (GYMOL) of the Universidad del Quindío.

2.2 Gas chromatography mass spectrometry analysis of WPO

The chemical composition of WPO was determined by gas chromatography mass spectrometry (GC-MS). An Agilent HP-6890N gas chromatograph coupled to an Agilent 5975N mass selective detector (Agilent Technologies, HP USA), equipped with a DM-1M capillary column (30 m long × 0.25 mm internal diameter and ×0.25 μm film thickness) was used. Helium (99.999%) was used as carrier gas at a flow rate of 1.0 mL min^{-1} and an injector temperature of 250 °C. WPO was diluted in propylene glycol and then 0.2 μL was injected in split mode (ratio 1 : 30). The oven temperature program was 70 °C for 10 min, increased to 100 °C at 5 °C min^{-1}, followed by an increase to 150 °C at 5 °C min^{-1}, then to 200 °C at 5 °C min^{-1} and finally to 250 °C at 5 °C min^{-1} for 15 min.

Mass spectra were recorded in electron impact ionization mode at 70 eV. The temperatures of the quadrupole mass detector, ion source and transfer line were set at 150, 230 and 280 °C, respectively. The identification of the compounds was based on mass spectra (MS) obtained with those from the NIST02.L, NIST5a.L and NIST98.L libraries and the selected ion monitoring mode was used to determine the concentrations of the compounds.

2.3 Film formulation

To obtain the films, the methodology proposed by Vargas *et al.*[21] was followed with some modifications. Initially, 3.6 g of cassava starch was added to 72 g of distilled water with constant stirring for 30 min and 600 rpm at 70 °C. In parallel, 2.4 g of sodium alginate was added to 72 g of distilled water at 60 °C with constant stirring for 30 min and 600 rpm (0.1% $CaCl_2$ was added for each gram of sodium alginate). Then, both solutions were mixed with constant stirring for 15 min.

Additionally, a 15% (w/w, with respect to the weight of cassava starch) glycerol solution was prepared by heating at 35 ± 5 °C for 15 min. Once the solutions were obtained, the percentages of WPO were added at a concentration of 0.5, 1.0 and 1.5% (w/w total solids). WPO was mixed with Tween 80 al 5% (w/w, based on WPO). Tween 80 was used as a non-ionic surfactant to stably disperse the dispersed oil phase droplets in the continuous water phase.

The film-forming solution (FFS) obtained was distributed on polystyrene Petri dishes (18 g) (64 cm^2) and dried in a forced air convection oven (Binder, FD – 115, Germany) at 45 °C ± 5 °C for 6 h. Film-forming solution (FFS) was prepared following the same methodology, without the addition of WPO. A control film (CF) was prepared following the same methodology, without adding WPO. All films were stored in a desiccator at 23 ± 2 °C and 50 ± 2% relative humidity (RH) for subsequent physical characterization. Fig. 1 shows the images of the films obtained.

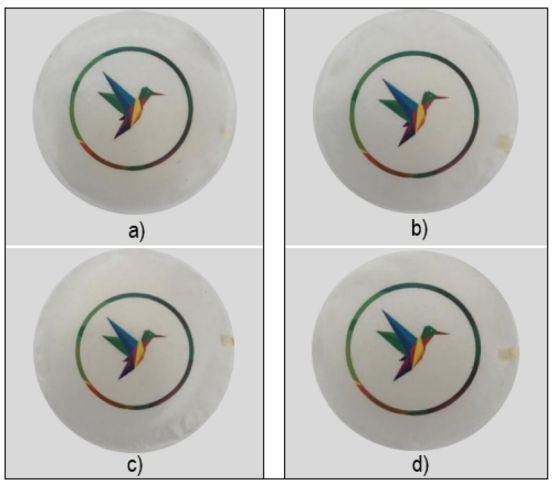

Fig. 1 Visual appearance of the films (a) CF, (b) FWPO 0.5%, (c) FWPO 1.0%, (d) FWPO 1.5%.

© 2024 The Author(s). Published by the Royal Society of Chemistry

Open Access Article. Published on 13 May 2024. Downloaded on 2/12/2026 11:27:03 PM. This article is licensed under a Creative Commons Attribution-NonCommercial 3.0 Unported Licence.

2.4 Antioxidant activity

The antioxidant activity of the obtained films was evaluated by 2,2-diphenyl-1-picryl-hydrazyl (DPPH) free radical scavenging assay, according to the methodology employed by M. Moradi *et al.*[22] with some modifications. Initially, 25 mg of film were immersed in 3 mL of deionized water, the obtained mixture was stirred at room temperature (25 °C) for 15 h; after this time, it was centrifuged at 4185*g* for 15 min. The obtained film extracts (2.8 mL) was mixed with 0.1 mL of 1 M methanol solution of DPPH, and left in the dark for 30 min at 25 °C.

The absorbance of the mixture was measured in a spectrophotometer at 515 nm; the absorbance of the solution without film (blank) was also measured. The percentage of inhibition or reduction of the DPPH radical from the radical scavenging activity of DPPH was calculated using eqn (1).

$$\mathrm{AA} = \frac{\mathrm{Abs_{DPPH}} - \mathrm{Abs_{filmextract}}}{\mathrm{Abs\ _{DPPH}}} \times 100 \quad (1)$$

where: AA (%) is the percentage inhibition or reduction of the DPPH radical, $\mathrm{Abs_{DPPH}}$ is the absorbance value at 515 nm of the methanolic solution of DPPH and film extract, Abs is the absorbance value at 515 nm for each formulated film.

2.5 Antimicrobial activity

The antimicrobial activity of the films obtained was determined using the agar disk diffusion method described by S.·K. Bajpai *et al.*[23] with some modifications *S. aureus* (ATCC 25923) and *E. coli* (ATCC 25922) stock cultures were kept at −80 °C until grown in tubes with Luria Bertani (LB) medium at 37 °C for 24 h, then in different tubes with LB at 37 °C for 12 h.

5 mm diameter disks of the films (previously sterilized on each side for 5 min with UV-C light: 254 nm) were placed in Petri dishes with solid Mueller–Hinton agar previously spread on the surface with 100 μL of 10^8 CFU mL^{-1} (according to McFarland's standard density of 0.5) suspensions with bacterial cultures of *S. aureus* (ATCC 25923) and *E. coli* (ATCC 25922). The Petri dishes were incubated at 37 °C for 24 h. The diameter of the inhibition zones of with respect to the weight of cassava starch the discs (mm) was measured using a digital caliper (Mitutoyo No. 192-30, Tokyo, Japan).

2.6 Thickness and mechanical properties

The thickness of the films was measured using a digital micrometer with an accuracy of 0.001 mm (Mitutoyo, Corp., Ltdy col., Tokyo, Japan). Ten measurements were taken at randomly selected points on each type of film obtained; the value of each thickness was the average of the measurements taken.

The mechanical properties of the films were measured on a texturometer (TA, XT2, Textura Technologies Corpy col., Scarsdale, NY, USA). Tensile strength (TS) and elongation at break (EB, %) were determined until rupture of the films. The samples were die-cut in the form of 2 cm × 6 cm sheets and conditioned for 48 h at 25 ± 0.2 °C and 50 ± 1% relative humidity. During analysis, they were subjected to tension with a 40 mm separation between the grips. Tensile strength and elongation were calculated according to the standard calculated according to ASTM D882-01 (ref. 24) of the American Society for Testing and Materials.

2.7 Water vapor permeability, moisture content, and solubility

To determine the water vapor permeability (WVP), the films were conditioned for 48 h at 20 ± 0.1 °C and a relative humidity of 40 ± 1%. It was evaluated according to ASTM E-96 (ref. 25) of the American Society for Testing and Materials. The capsules were weighed every hour for 9 h to determine the weight loss of the films.

Moisture content was determined by gravimetric method,[26] conditioning for 48 h at 25 °C at 50% relative humidity. The samples were cut into 2 cm × 2 cm sheets and weighed. Initially, the weight of the films (W_m) was taken, subsequently they were placed on a drying in a forced air convection oven (Binder, FD – 115, Germany) at 105 °C for 24 h to a constant weight (W_d). The moisture content was calculated using eqn (2).

$$\mathrm{Moisture\ \ content} = \frac{W_m - W_d}{W_d} \times 100 \quad (2)$$

The solubility of films was determined by the percentage of the film dry matter that is soluble in water. The methodology reported by R. Akhter *et al.*[27] was followed with some modifications. The films were cut into 2 cm × 2 cm sheets. The samples were dried at 105 °C to constant weight to obtain the initial dry mass (M_1). The films were placed in 50 mL of distilled water, covered, and stored at 25 °C for 24 h, then vacuum filtered and dried at 105 °C to constant weight to obtain the final dry mass (M_2). Solubility was calculated using eqn (3).

$$\mathrm{Film\ solubility\ (\%)} = \frac{M_1 - M_2}{M_1} \times 100 \quad (3)$$

2.8 Color and opacity

The color evaluation of the films was performed with a Minolta CM-2002R photocolorimeter (Minolta Camera Coy col., Osaka, Japan), using a D65 illuminant and a 10° standard observer.[28] The determination and expression of the color were performed based on CIEL*a*b* coordinates and reflectance values.[29] The Luminosity (L*), red-green (a*), and yellow-blue (b*) parameters were obtained directly from the equipment.

Film opacity was determined according to U. Siripatrawan and B. R. Harte.[30] Film samples were cut into rectangular pieces (2 cm × 7 cm) and placed directly on a spectrophotometer (Evolution 60S, Thermo Scientific, Pittsburgh, PA, USA), then the absorbance of the film was measured at $\lambda = 600$ nm. The opacity was calculated using eqn (4).

$$\mathrm{Opacity} = \frac{\mathrm{Abs_{600}}}{X} \quad (4)$$

where Abs 600 is the absorbance at 600 nm and X is the film thickness (mm).

Open Access Article. Published on 13 May 2024. Downloaded on 2/12/2026 11:27:03 PM. This article is licensed under a Creative Commons Attribution-NonCommercial 3.0 Unported Licence.

2.9 X-ray diffraction (XRD)

The XRD patterns of the obtained films were analyzed on a D8 Advance X-ray diffractometer (Bruker AXS, Germany) with Co Kα radiation of 1.544 nm wavelength at 40 kV and 15 mA. The film samples were scanned in the diffraction angle range (2θ) from 5° to 60° with a step size of 0.02°. The relative crystallinity was calculated by dividing the crystalline area by the total area.

2.10 Fourier transformed infrared spectroscopy

The optical characterization of the films was performed by Fourier transform infrared spectroscopy (FTIR). The spectra of the samples were obtained in wavenumber ranges from 4000 to 400 cm^{-1} using a PerkinElmer Spectrum (Mod. Spectrum Two, Waltham, MA, USA) equipped with a single-reflection diamond crystal ATR module. Spectra were recorded at a spectral range between 400 and 4000 cm^{-1} at a scan rate of 32 scans and spectral resolution of 4 cm^{-1}.

2.11 Scanning electron microscopy (SEM)

The morphology of the films was analyzed by scanning electron microscopy (JEOL model JSM-6610LV, Japan). Samples of 4 mm × 4 mm were used to obtain images of the surface and cross-section of the films. The images were captured with an accelerating voltage of 5 kV and observed at 1000× magnification. All samples were coated with gold before observation.

2.12 Statistical analysis

Statistical analysis of the data was performed using analysis of variance (ANOVA), using the Statgraphics Centurion XVIII program. Data were classified and statistical differences were evaluated in ranges with one-way analysis of variance ANOVA and Tukey multiple comparison tests. All cases were considered significant to have a value of $p < 0.05$. All experiments were carried out in triplicate.

3. Results and discussion

3.1 Chemical composition of WPO

The chemical composition of WPO is presented in Table 1. According to the GC-MS analysis, 9 compounds were found, of which piperine (48.02%), α-pinene (15.10%), limonene (10.09%) and α-caryophyllene (9.83%) were identified as the main compounds. The alkaloid piperine is considered the most important compound present in WPO, due to its antioxidant, anti-inflammatory, therapeutic, and antimicrobial action.[31]

Furthermore, *P. nigrum* has been shown to have a diverse content of secondary metabolites.[32] These variations in chemical composition are common in extracts obtained from plant matrices, as secondary metabolites are affected by seasonal, geographical, nutritional factors and extraction processes.[33]

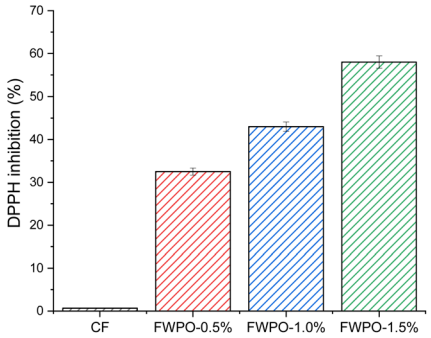

Fig. 2 DPPH inhibition activity of the films containing or not different concentrations of white pepper oleoresin (WPO).

3.2 Antioxidant activity

The incorporation of WPO produced a significant increase ($p < 0.05$) in the antioxidant properties of all films compared to CF (Fig. 2). These results are attributed to the presence of piperine, a secondary metabolite to which antimutagenic and antioxidant properties have been attributed, due to the presence of phenolic compounds and flavonoids.[34] It also presents monoterpenes (see Table 1) such as α-pinene, α-caryophyllene, and limonene, to which antioxidant properties have also been attributed.

3.3 Antimicrobial activity

The antimicrobial activity of the films obtained with different concentrations of WPO against *E. coli* and *S. aureus* is shown in Table 2 and Fig. 3. CF did not present an inhibition zone. FWPOs showed a significant increase ($P < 0.05$) in antibacterial activity. FWPO 0.5%, FWPO 1.0% and FWPO 1.5% showed zone of inhibition against *E. coli* (11.80, 12.25 and 13.56) and *S. aureus* (12.81, 13.23 and 14.56).

Table 1 Compounds identified in white pepper oleoresin (*Piper nigrum* L.)

Compound	Retention time (min)	Relative content (%)
Bicyclo[3.1.1]hept-2-ene, 3,6,6-trimethyl	6.07	2.70
1-Pentene, 5-methoxy	6.45	2.44
Limonene	13.56	10.09
3-Buten-2-one, 4-(2,5,6,6-tetramethyl-2-cyclohexen-1-yl)	16.43	6.43
α-Pinene	10.30	15.10
α-Caryophyllene	19.85	9.83
Triacetin	16.69	1.62
Bicyclo[5.2.0]nonane, 2-methylene-4,8,8-trimethyl-4-vinyl-	18.89	2.35
Piperine	60.63	48.02

© 2024 The Author(s). Published by the Royal Society of Chemistry

Open Access Article. Published on 13 May 2024. Downloaded on 2/12/2026 11:27:03 PM. This article is licensed under a Creative Commons Attribution-NonCommercial 3.0 Unported Licence.

Table 2 Antibacterial activity of the films containing or not different concentrations of white pepper oleoresin (WPO) against *E. coli* and *S. aureus*[a]

	Zona de inhibición (mm)	
Film	*E. coli*	*S. aureus*
CF	0.0[a]	0.0[a]
FWPO 0.5%	11.8 ± 1.05[b]	12.81 ± 1.12[b]
FWPO 1.0%	12.25 ± 1.21[b]	13.23 ± 1.17[b]
FWPO 1.5%	13.56 ± 1.13[c]	14.56 ± 1.13[c]

[a] Data reported are mean values ± standard deviation. The medians in the same column with different letters are significantly different (Tukey: $p < 0.05$).

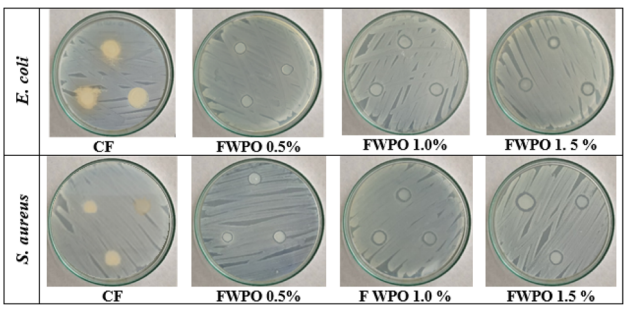

Fig. 3 Antibacterial activity of the films containing or not different concentrations of white pepper oleoresin (WPO) against *E. coli* and *S. aureus*.

The results revealed a slightly higher sensitivity to *S. aureus* compared to *E. coli*, indicating a higher susceptibility of Gram-positive bacteria to WPO in contrast to Gram-negative bacteria. This difference could be attributed to the structure of the cell wall, since Gram-negative bacteria possess a thin peptidoglycan layer and their outer cell membrane is composed of lipoproteins.[35] Additionally, piperine has been reported to interact and disintegrate membranes, inhibiting the formation of bacterial colonies.[32]

3.4 Thickness and mechanical properties

The results obtained for the thickness of the film are presented in Table 3. The values obtained did not present significant changes, ($p > 0.05$). Similar results were observed for corn starch films with Zataria multiflora oil.[38]

The addition of WPO to the films had a significant effect ($p < 0.05$) on the mechanical properties (Table 3). Tensile strength (TS) increased, while elongation at break (EB) decreased with increasing WPO concentration, compared to CF. This indicates that the incorporation of WPO reduces the volume of free space in the polymeric matrix, strengthens the films and forms more homogeneous and compact structures.

This should be attributed to the presence of several additional functional groups, such as hydroxyl, ketone, and ester groups in WPO components, which can form stronger interactions between the components of the film-forming solution.[39] The increase in TS and the decrease in EB values were similar to the results of A. A. Marzlan *et al.*[40]

In addition, the mechanical properties of the films were compared with biodegradable polymers (PLA and PHB) and thermoplastic polymers (PP and PET) reported in the literature. Although the elongation at break of polylactic acid (PLA) and poly (3-hydroxybutyrate) (PHB) is low compared to PP and PET, it has been shown that when blended with other compounds it has allowed to improve the elongation at break.[36] Therefore, FWPOs are less flexible and stretchable than conventional polymers.

3.5 Water vapor permeability, moisture content and solubility

Water vapor permeability (WVP) and moisture content of CF were 58.62 g h^{-1} m^{-2} and 12.32%, respectively, on the contrary, a significant decrease ($p < 0.05$) in WVP and moisture content was observed as the concentration of WPO in the films increased (Table 4). This suggests that the addition of WPO confers hydrophobic properties to the films, preventing the adsorption and desorption of water molecules due to interactions between oleoresin and the other components of the film, which reduce the moisture content and the availability of hydrophilic groups, resulting in improved barrier properties of the films.[41] However, PLA, PHB, PP and PET polymers present a lower WPV than the values obtained in this research.

Regarding the solubility of the films, a significant decrease ($p < 0.05$) was observed with the addition of WPO in the films compared to CF. This is attributed to lipid–polysaccharide interactions through hydrogen bonds, which limit the

Table 3 Thickness and mechanical properties of the films containing or not different concentrations of white pepper oleoresin (WPO)[a]

Film	Thickness (mm)	TS (MPa)	EB (%)
CF	0.152 ± 0.01[NS]	7.85 ± 0.44[a]	18.22 ± 0.82[a]
FWPO 0.5%	0.149 ± 0.06	9.73 ± 0.24[b]	17.76 ± 0.47[a]
FWPO 1.0%	0.153 ± 0.02	12.67 ± 0.40[c]	16.45 ± 0.55[b]
FWPO 1.5%	0.160 ± 0.03	14.67 ± 1.60[d]	15.83 ± 0.73[c]
PLA	—	44–60 (ref. 36 and 37)	<6–30.7 (ref. 36 and 37)
PHB	—	40 (ref. 36)	5 (ref. 36)
PP	—	40–50 (ref. 37)	100 (ref. 37)
PET	—	61.67 (ref. 37)	140–275 (ref. 37)

[a] NS, not significantly different. Data reported are mean values ± standard deviation. The medians in the same column with different letters are significantly different (Tukey: $p < 0.05$).

Open Access Article. Published on 13 May 2024. Downloaded on 2/12/2026 11:27:03 PM. This article is licensed under a Creative Commons Attribution-NonCommercial 3.0 Unported Licence.

Table 4 Water vapor permeability (WVP), humidity and solubility of the films containing or not different concentrations of white pepper oleoresin (WPO)[a]

Film	WVP (g m^{-2} h^{-1})	Humidity (%)	Solubility (%)
CF	58.62 ± 1.65[a]	12.32 ± 0.35[a]	54.18 ± 1.25[a]
FWPO 0.5%	48.86 ± 1.45[b]	11.20 ± 0.54[b]	50.36 ± 1.56[b]
FWPO 1.0%	41.36 ± 1.87[c]	9.64 ± 0.42[c]	42.14 ± 1.36[c]
FWPO 1.5%	35.25 ± 1.57[d]	8.34 ± 0.35[d]	34.25 ± 1.65[d]
PLA	1.13–2.08 (ref. 37)	—	—
PHB	0.05 (ref. 37)	—	—
PP	0.39–0.46 (ref. 37)	—	—
PET	1.33 (ref. 37)	—	—

[a] Data reported are mean values ± standard deviation. The medians in the same column with different letters are significantly different (Tukey: $p < 0.05$).

interactions of hydroxyl groups with the molecules by decreasing their availability, leading to the formation of more water-resistant films.[27] Similar results were observed in corn starch and chitosan films incorporated with essential oil of nettle.[42]

3.6 Color and opacity

The values of the color parameters (L^*, a^* and b^*) and the opacity of the films are shown in Table 5. No significant differences were observed between the values of a^*. Lightness (L^*) decreased significantly ($p < 0.05$) as the concentration of WPO increased; in contrast, the value of the parameter b^* (blue/yellow) increased significantly ($p < 0.05$) compared to CF. These changes are attributed to the nature of the compounds used in the formulation. Similar results were observed in corn starch films incorporated with Thymus vulgaris essential oil.[43]

Opacity was used to evaluate the transparency of the film, where a lower opacity indicates a higher transparency. CF exhibited the lowest opacity (0.38). The addition of WPO significantly ($P < 0.05$) increased the opacity of the films. FWPO 0.5%, FWPO 1.0% and FWPO 1.5% presented opacity values 0.47, 0.67 and 0.93, respectively. FWPO 1.5% had the highest opacity value. Opacity is directly related to the degree of film homogeneity and higher film opacity can be a desirable property for food packaging when foods are light sensitive, as it provides an excellent barrier against visible light and helps prevent light-induced lipid oxidation.[44]

3.7 X-ray diffraction (XRD)

The X-ray diffractograms of the films are shown in Fig. 4. The FWPOs showed mild peaks at $2\theta = 16°$, 23.5° and 25.4°, a broad peak at 14° and a peak with high intensity at $2\theta = 20.3°$ related to glycerol, however, FWPOs presented the highest intensity in this peak, suggesting a higher crystallinity (47.1% for FWPO 1.5%) of the polymer that is favored by the interaction between glycerol, starch, alginate and WPO molecules. In one study it was reported that the addition of thyme oil increased the crystallinity of chitosan/gum arabic based films.[45]

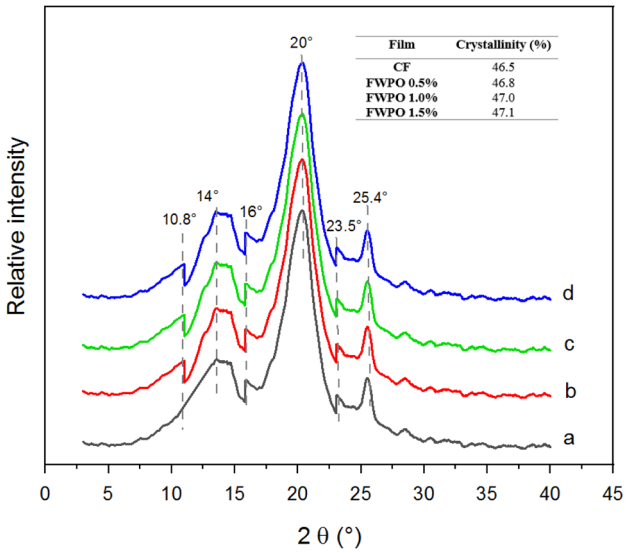

Fig. 4 XRD patterns of the films (a) CF (b) FWPO 0.5%, (c) FWPO 1.0%, (d) FWPO 1.5%.

It is noteworthy that also in FWPOs a slight peak appeared at 10.8°, which could indicate a cross-linking between WPO lipids with starch and sodium alginate.[27] Furthermore, the addition of WPO does not affect the structural uniformity of the film-forming solution as observed in SEM images (Fig. 6). Similar results were reported for cassava starch-based films, where the formation of new peaks was observed upon incorporation of cinnamon essential oil.[38] In another study, it was observed in pectin films that the incorporation of marjoram essential oil caused the appearance of a new peak and did not alter the crystalline structure.[47]

3.8 Fourier transformed infrared (FTIR) spectroscopy

The FTIR spectra are presented in Fig. 5, showing the functional groups and intermolecular interactions of the film components. The bands between 3630 and 3011 cm^{-1} are related to the stretching of hydroxyl groups present in the films.[48] The bands

Table 5 CIELAB color parameters and opacity of the films containing or not different concentrations of white pepper oleoresin (WPO)[a]

Film	L^*	a^*	b^*	Opacity
CF	94.52 ± 0.52[a]	−1.24 ± 0.57[a]	2.56 ± 0.12[a]	0.38 ± 0.05[a]
FWPO 0.5%	91.22 ± 0.55[b]	−1.52 ± 0.66[a]	4.65 ± 0.42[b]	0.47 ± 0.01[b]
FWPO 1.0%	90.63 ± 0.65[b]	−1.48 ± 0.57[a]	4.83 ± 0.22[b]	0.67 ± 0.03[c]
FWPO 1.5%	88.57 ± 0.72[c]	−1.57 ± 0.72[a]	4.98 ± 0.45[b]	0.93 ± 0.02[d]

[a] Data reported are mean values ± standard deviation. The medians in the same column with different letters are significantly different (Tukey: $p < 0.05$).

© 2024 The Author(s). Published by the Royal Society of Chemistry

Open Access Article. Published on 13 May 2024. Downloaded on 2/12/2026 11:27:03 PM.
This article is licensed under a Creative Commons Attribution-NonCommercial 3.0 Unported Licence.

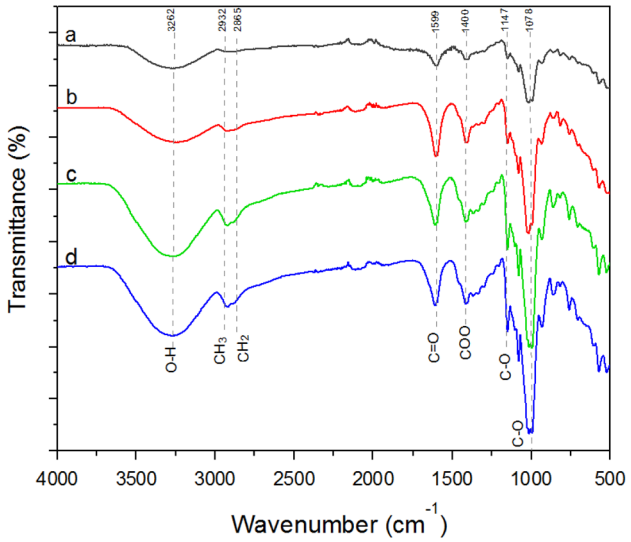

Fig. 5 FTIR spectra of the films (a) CF, (b) FWPO-0.5%, (c) FWPO 1.0%, (d) FWPO 1.5%.

at 2932 and 2865 cm^{-1} correspond to antisymmetric and symmetric stretching frequencies of $-CH_3$ and $-CH_2$ bonds. Changes in the intensity of these bands were observed as the concentration of WPO in the films increases, which could be attributed to an increase in the content of the ester group associated with the C–H bond present in the WPO molecule.

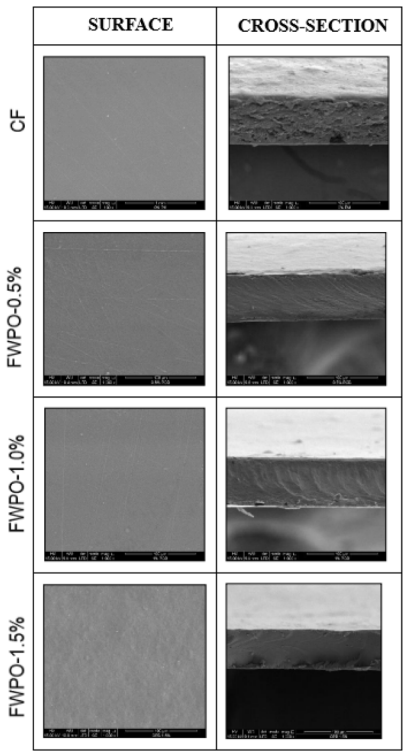

Fig. 6 SEM images of the surface (left column) and the cross-sections (right column) of the films containing or not different concentrations of white pepper oleoresin (WPO).

Similar results were reported by Y. Zhou *et al.*[46] on cassava starch-based films with cinnamon essential oil.

The band at 2109 cm^{-1} (=CO stretching) of carboxylic acids.[49] The vibrational frequencies at 1599 and 1400 cm^{-1} correspond to the bending and stretching vibrations of the O–H groups of matrix-bound water.[50] Furthermore, these bands have been associated with symmetric and asymmetric stretching vibrations of the C–O bond of the –COO group.[51] However, changes in the intensity and length of these bands were observed upon incorporation of WPO in the films, caused by the vibration of the aromatic ring of phenolic compounds.[52]

The stretching frequencies of the C–O bonds in the C–O–C chains are associated with the bands identified at 1147 and 1078 cm^{-1}, while the stretching vibration of the pyranose ring is related to the band located at 994 cm^{-1}.[53,54] The observed changes in the position of the absorption bands at 1100, 1009 cm^{-1}, indicate a possible interaction between the hydrogen bonds present in starch, alginate, and WPO. In the region below 800 cm^{-1}, the spectra are associated with skeletal vibrations of the glucopyranose rings.[55]

3.9 Scanning electron microscopy (SEM)

SEM images of the surface and cross-section of the obtained films are presented in Fig. 6. In general, the films showed a smooth, uniform and homogeneous surface without pore formation, cracks, or fractures. While in cross section, the CF exhibited a rough and non-uniform appearance.

The FWPOs presented a continuous, homogeneous laminar appearance and no evidence of separation of the WPO droplets was observed, indicating a good interaction and compatibility between the WPO and the rest of the polymeric matrix components. These results agree with the mechanical properties, FTIR, and XRD analyses. Similar results were found by S. Acosta *et al.*[56] in starch and gelatin-based films observing a heterogeneous and irregular structure.

4. Conclusions

In this work, piperine was identified as the main component of white pepper oleoresin (WPO). FWPOs showed bacteriostatic activity against *S. aureus* and *E. coli* microorganisms. The increase in WPO incorporation influenced the color change, obtaining films with a reduction in gloss, a tendency toward yellow (by increasing the b^* values) and an increase in opacity.

In addition, a decrease in water vapor permeability (WVP), elongation at break (EB), moisture content, and solubility were observed as the concentration of WPO in the films increased. In contrast, tensile strength (TS) increased and thickness was not affected. SEM, FTIR and XRD analyzes confirmed the intermolecular interactions between white pepper oleoresin, starch, sodium alginate, and glycerol. Finally, the FWPOs presented a percentage of DPPH removal between 32.5 and 58%. These results indicate the potential viability of the films for food packaging applications.

Therefore, FWOP 1.5% is proposed to be used as a food packaging material due to its mechanical, physical, optical,

Open Access Article. Published on 13 May 2024. Downloaded on 2/12/2026 11:27:03 PM. This article is licensed under a Creative Commons Attribution-NonCommercial 3.0 Unported Licence.

structural, antibacterial and antioxidant properties obtained through this research.

Author contributions

Olga Lucía Torres Vargas – funding acquisition, conceptualization, writing – reviewing and editing; Iván Andrés Rodríguez Agredo – supervision, methodology, data curation and conceptualization; Yessica Viviana Galeano Loaiza – formal analysis, methodology, investigation, validation and writing.

Conflicts of interest

There are no conflicts to declare.

Acknowledgements

We would like to thank the Vicerrectoria de Investigaciones at Universidad del Quindío for providing financial support (Research Project no. 1073).

Notes and references

1 J. C. da Costa, K. S. Miki, A. da Silva Ramos and B. E. Teixeira-Costa, *Heliyon*, 2020, **6**, e03718.
2 A. Kumar, M. Hasan, S. Mangaraj, M. Pravitha, D. K. Verma and P. P. Srivastav, *Appl. Food Res.*, 2022, **2**, 100118.
3 L. Almasi, M. Radi, S. Amiri and D. J. McClements, *Food Hydrocolloids*, 2021, **117**, 106733.
4 L. Y. Maroufi, M. Tabibiazar, M. Ghorbani and A. Jahanban-Esfahlan, *Int. J. Biol. Macromol.*, 2021, **187**, 179–188.
5 World Health Organization (WHO), *Key Facts on Food Safety*, 2020, cited 20 November 2023, available from: **https://www.who.int/es/news-room/fact-sheets/detail/food-safety**.
6 C. V. Dhumal, J. Ahmed, N. Bandara and P. Sarkar, *Food Packag. Shelf Life*, 2019, **21**, 100380.
7 M. C. Pellá, O. A. Silva, M. G. Pellá, A. G. Beneton, J. Caetano, M. R. Simões and D. C. Dragunski, *Food Chem.*, 2020, **309**, 125764.
8 J. Orozco-Parra, C. M. Mejía and C. C. Villa, *Food Hydrocolloids*, 2020, **104**, 105754.
9 A. Martău, M. Mihai and C. Vodnar, *Polymers*, 2019, **11**, 1837, DOI: **10.3390/polym11111837**.
10 M. Hasan, A. Kumar, C. Maheshwari and S. Mangraj, *Int. J. Chem. Stud.*, 2020, **8**, 2242–2245.
11 M. Meghwal and T. K. Goswami, *Phytother. Res.*, 2013, **27**, 1121–1130.
12 J. Rakmai, B. Cheirsilp, J. C. Mejuto, A. Torrado-Agrasar and J. Simal-Gándara, *Food Hydrocolloids*, 2017, **65**, 157–164.
13 K. J. Figueroa-Lopez, M. M. Andrade-Mahecha and O. L. Torres-Vargas, *Food Packag. Shelf Life*, 2018, **17**, 50–56.
14 N. Ozdemir, C. C. Pola, B. N. Teixeira, L. E. Hill, A. Bayrak and C. L. Gomes, *LWT–Food Sci. Technol.*, 2018, **91**, 439–445.
15 E. Xie, Y. Chen, W. Yang, Q. Pan, J. Z. Shen, F. Zhou, J. Shen, T. Lao, Q. Li and X. Li, *Food Res. Int.*, 2024, **184**, 114205.
16 Food and Drug Administration (FDA), cited 19 April 2024, Available from: **https://www.accessdata.fda.gov/scripts/cdrh/cfdocs/cfcfr/cfrsearch.cfm?fr=172.840**.
17 STAN, *Codex. Stan 192-1995, Norma general del Codex para los aditivos alimentarios*, FAO, Roma, 2010.
18 B. Chassaing, O. Koren, J. K. Goodrich, A. C. Poole, S. Srinivasan, R. E. Ley and A. T. Gewirtz, *Nature*, 2015, **519**(7541), 92–96.
19 C. Kriegel, M. Festag, R. S. Kishore, D. Roethlisberger and G. Schmitt, *Children*, 2019, **7**(1), 1.
20 A. N. Adilah, B. Jamilah, M. A. Noranizan and Z. N. Hanani, *Food Packag. Shelf Life*, 2018, **16**, 1–7.
21 O. L. Vargas, Y. V. Loaiza and M. L. Gonzalez, *J. Mater. Res. Technol.*, 2021, **13**, 2239–2250.
22 M. Moradi, H. Tajik, S. M. Rohani and A. Mahmoudian, *LWT–Food Sci. Technol.*, 2016, **72**, 37–43.
23 S. K. Bajpai, N. Chand and V. Chaurasia, *Food Bioprocess Technol.*, 2012, **5**, 1871–1881.
24 ASTM, Standard test method for tensile properties of thin plastic sheeting, in *Standard Designations D882-01, Annual Book of ASTM Standards*, American Society for Testing and Materials, Philadelphia, PA, 2002.
25 ASTM, Standard test methods for water vapor transmission of materials, in *E96 e 05, Annual Book of ASTM Standards*, American Society for Testing and Materials, 2005.
26 AOAC Association of Official Agricultural Chemists, *Official Methods of Analysis of AOAC International*, AOAC International Rockville, USA, 20th edn, 2016.
27 R. Akhter, F. A. Masoodi, T. A. Wani and S. A. Rather, *Int. J. Biol. Macromol.*, 2019, **137**, 1245–1255.
28 UNE 40-080, *Determinación de las magnitudes cromáticas CIE, Norma española*, Instituto Español de Normalización (IRANOR), Madrid, 1984.
29 CIE, *Industrial Colour-Difference Evaluation, Technical Report 116/1995*, Commission Internationale de I'Eclairage Central Bureau, Vienna, Austria, 1995.
30 U. Siripatrawan and B. R. Harte, *Food Hydrocolloids*, 2010, **24**, 770–775.
31 S. Shityakov, E. Bigdelian, A. A. Hussein, M. B. Hussain, Y. C. Tripathi, M. U. Khan and M. A. Shariati, *Eur. J. Med. Chem.*, 2019, **176**, 149–161.
32 B. Salehi, Z. A. Zakaria, R. Gyawali, S. A. Ibrahim, J. Rajkovic, Z. K. Shinwari, T. Khan, J. Sharifi-Rad, A. Ozleyen, E. Turkdonmez, M. Valussi, T. B. Tumer, L. M. Fidalgo, M. Martorell and W. N. Setzer, *Molecules*, 2019, **24**, 1364.
33 Y. Li, D. Kong, Y. Fu, M. R. Sussman and H. Wu, *Plant Physiol. Biochem.*, 2020, **148**, 80–89.
34 I. U. Haq, M. Imran, M. Nadeem, T. Tufail, T. A. Gondal and M. S. Mubarak, *Phytother. Res.*, 2021, **35**, 680–700.
35 J. A. Lepe and L. Martínez-Martínez, *Medicina Intensiva*, 2022, **46**, 392–402.
36 L. Jiang and J. Zhang, Plastics Design Library, in *Applied Plastics Engineering Handbook*, 2011, pp. 145–158, ISBN 9781437735147, DOI: **10.1016/B978-1-4377-3514-7.10009-1**.
37 S. Shaikh, M. Yaqoob and P. Aggarwal, *Curr. Res. Food Sci.*, 2021, **202**(4), 503–520.

© 2024 The Author(s). Published by the Royal Society of Chemistry

Open Access Article. Published on 13 May 2024. Downloaded on 2/12/2026 11:27:03 PM.
This article is licensed under a Creative Commons Attribution-NonCommercial 3.0 Unported Licence.

38 E. Amiri, M. Aminzare, H. H. Azar and M. R. Mehrasbi, *Meat Sci.*, 2019, **153**, 66–74.
39 X. L. Li, Y. Shen, F. Hu, X. X. Zhang, K. Thakur, K. R. Rengasamy, M. R. Khan, R. Busquets and Z. J. Wei, *Int. J. Biol. Macromol.*, 2023, **242**, 124767.
40 A. A. Marzlan, B. J. Muhialdin, N. H. Abedin, N. Manshoor, F. H. Ranjith, A. Anzian and A. S. Hussin, *Ind. Crops Prod.*, 2022, **184**, 115058.
41 B. Wang, J. Sui, B. Yu, C. Yuan, L. Guo, A. M. Abd El-Aty and B. Cui, *Carbohydr. Polym.*, 2021, **254**, 117314.
42 F. Kalateh-Seifari, S. Yousefi, H. Ahari and S. H. Hosseini, *Polymers*, 2021, **13**, 2113.
43 N. Ardjoum, N. Chibani, S. Shankar, S. Salmieri, H. Djidjelli and M. Lacroix, *Int. J. Biol. Macromol.*, 2023, **224**, 578–583.
44 X. Sun, H. Zhang, J. Wang, M. Dong, P. Jia, T. Bu, Q. Wang and L. Wang, *Food Packag. Shelf Life*, 2021, **29**, 100741.
45 R. Zhao, J. Chen, S. Yu, R. Niu, Z. Yang, H. Wang, H. Cheng, X. Ye, D. Liu and W. Wang, *Food Hydrocolloids*, 2023, **134**, 108094.
46 Y. Zhou, X. Wu, J. Chen and J. He, *Int. J. Biol. Macromol.*, 2021, **184**, 574–583.
47 H. Almasi, S. Azizi and S. Amjadi, *Food Hydrocolloids*, 2020, **99**, 105338.
48 B. Pfister and S. C. Zeeman, *Cell. Mol. Life Sci.*, 2016, **73**, 2781–2807.
49 S. N. Mousavi, H. Daneshvar, M. S. Dorraji, Z. Ghasempour, V. Panahi-Azar and A. Ehsani, *Mater. Chem. Phys.*, 2021, **267**, 124583.
50 M. Zhang and H. Chen, *Int. J. Biol. Macromol.*, 2023, **233**, 123462.
51 D. Alves, M. A. Cerqueira, L. M. Pastrana and S. Sillankorva, *Food Res. Int.*, 2020, **128**, 108791.
52 M. Kaya, P. Ravikumar, S. Ilk, M. Mujtaba, L. Akyuz, J. Labidi, A. M. Salaberria, Y. S. Cakmak and S. K. Erkul, *Innovative Food Sci. Emerging Technol.*, 2018, **45**, 287–297.
53 K. M. Dang and R. Yoksan, *Carbohydr. Polym.*, 2015, **115**, 575–581.
54 T. J. Gutiérrez, L. A. Toro-Márquez, D. Merino and J. R. Mendieta, *Food Hydrocolloids*, 2019, **89**, 283–293.
55 A. Hejna, J. Lenża, K. Formela and J. Korol, *J. Polym. Environ.*, 2019, **27**, 1112–1126.
56 S. Acosta, A. Chiralt, P. Santamarina, J. Rosello, C. González-Martínez and M. Cháfer, *Food Hydrocolloids*, 2016, **61**, 233–240.